0026-895X/08/7405-1319–1332$20.00
MOLECULAR PHARMACOLOGY
Copyright © 2008 The American Society for Pharmacology and Experimental Therapeutics
Mol Pharmacol 74:1319–1332, 2008

Vol. 74, No. 5
48793/3400212
Printed in U.S.A.

Mitochondrial Respiratory Enzyme Complexes in Rostral Ventrolateral Medulla as Cellular Targets of Nitric Oxide and Superoxide Interaction in the Antagonism of Antihypertensive Action of eNOS Transgene[S]

Ling-Chang Kung, Samuel H. H. Chan, Kay L. H. Wu, Chen-Chun Ou, Ming-Hon Tai, and Julie Y. H. Chan

Department of Neurology, Antai Tian-Sheng Memorial Hospital, Pintong, Taiwan, Republic of China (L.-C.K.); Center for Neuroscience, National Sun Yat-sen University, Kaohsiung, Taiwan, Republic of China (S.H.H.C., K.L.H.W.); and Department of Medical Education and Research, Kaohsiung Veterans General Hospital, Kaohsiung, Taiwan, Republic of China (C.-C.O., M.-H.T., J.Y.H.C.)

Received May 12, 2008; accepted August 19, 2008

ABSTRACT

Overproduction of nitric oxide (NO) by gene transduction of endothelial NO synthase (eNOS) in rostral ventrolateral medulla (RVLM), which is responsible for maintenance of vasomotor tone, reduces arterial pressure in spontaneously hypertensive rats (SHR). This NO-induced vasodepression, however, is not sustained and is followed by rebound hypertension. Because superoxide anion ($O_2^{\cdot-}$) level is increased and synthesis or activity of mitochondrial manganese superoxide dismutase (SOD2) is reduced in RVLM during hypertension, we hypothesized that an interaction between NO and $O_2^{\cdot-}$ in RVLM, using mitochondrial respiratory enzyme complexes (MRC) as the cellular target, contributes to those cardiovascular outcomes after eNOS gene transduction in SHR. The present study assessed this hypothesis using adenoviral vectors to overexpress eNOS (AdeNOS) and/or SOD2 (AdSOD2) in RVLM of SHR or normotensive Wistar-Kyoto (WKY) rats. Microinjection of AdeNOS bilaterally into RVLM elicited 35% depression of MRC-I enzyme activity and evoked 60% and 50% increase in $O_2^{\cdot-}$ and peroxynitrite level in RVLM of SHR, but not WKY rats, which was reversed by cotransduced AdSOD2 or treatment with peroxynitrite decomposition catalyst. Cotransduction of AdeNOS and AdSOD2 in RVLM of SHR elicited significantly greater decreases in arterial pressure and heart rate than those promoted by the individual transgene and prevented the AdeNOS-induced rebound hypertension. We conclude that an interactive action between NO and $O_2^{\cdot-}$ on MRC-I in RVLM via formation of peroxynitrite contributes to the unsustained hypotensive effects of NO after overexpression of eNOS in SHR. The mitochondria-derived $O_2^{\cdot-}$ also mediates the rebound hypertension induced by eNOS transgene in RVLM of SHR.

Nitric oxide (NO) is a gaseous molecule that plays an active role in central cardiovascular regulation (Zanzinger, 1999). One brain region in which NO is of pivotal importance in this regulatory machinery is the rostral ventrolateral medulla (RVLM) (Chan et al., 2001; Mayorov, 2005), which provides tonic sympathetic outflow for the maintenance of vasomotor tone (Dampney, 1994). Accumulating evidence suggests that NO deficiency in the RVLM may underlie sympathetic overexcitation (Kagiyama et al., 1998; Chan et al., 2003; Tandai-Hiruma et al., 2005) or impaired baroreflex regulation (Kishi et al., 2003) during hypertension. Accordingly, overproduction of NO by gene transduction of endothelial nitric-oxide

This study was supported by research grants NSC-97-2752-B-110-001-PAE (S.H.H.C.) and NSC-97-2752-B075-B-001-PAE (M.H.T., J.Y.H.C.) from National Science Council, and VGHKS 96G-21 from Kaohsiung Veterans General Hospital (J.Y.H.C.), Taiwan, Republic of China.

Article, publication date, and citation information can be found at http://molpharm.aspetjournals.org.

doi:10.1124/mol.108.048793.

[S] The online version of this article (available at http://molpharm.aspetjournals.org) contains supplemental material.

ABBREVIATIONS: NO, nitric oxide; RVLM, rostral ventrolateral medulla; eNOS, endothelial nitric-oxide synthase; MRC, mitochondrial respiratory enzyme complex; UCP-2, uncoupling protein-2; SOD1, copper/zinc superoxide dismutase; SOD2, manganese superoxide dismutase; SOD3, extracellular superoxide dismutase; SHR, spontaneously hypertensive rat; AdeNOS, adenoviral vectors encoding endothelial nitric-oxide synthase; AdSOD2, adenoviral vectors encoding manganese superoxide dismutase; WKY, Wistar-Kyoto; GFP, green fluorescence protein; AdGFP, adenoviral vectors encoding green fluorescence protein; Adβgal, adenoviral vectors encoding β-galactosidase; pfu, plaque-forming unit; CoQ_{10}, coenzyme Q_{10}; NOS, nitric-oxide synthase; L-NAME, N^{ω}-nitro-L-arginine-methyl ester; L-NIO, N^5-(1-iminoethyl)-L-ornithine; FeTMPyP, 5,10,15,20-tetrakis-(*N*-methyl-4′-pyridyl)-porphyrinato iron (III); aCSF, artificial cerebrospinal fluid; MSAP, mean systemic arterial pressure; HR, heart rate; NCCR, NADH cytochrome *c* reductase; SCCR, succinate cytochrome *c* reductase; nNOS, neuronal nitric-oxide synthase; iNOS, inducible nitric-oxide synthase; RT, reverse transcription; PCR, polymerase chain reaction; CCO, cytochrome *c* oxidase.

synthase (eNOS) in the RVLM promotes sympathoinhibition and depressor response (Kishi et al., 2002; Tai et al., 2005) and improves the impaired baroreflex control of heart rate (Kishi et al., 2003) in hypertensive rats. The antihypertensive effects of eNOS gene transduction, however, fail to provide a sustained normalization of arterial pressure (Kishi et al., 2002; Tai et al., 2005) and are followed by rebound hypertension (Tai et al., 2005). The cellular mechanisms for those intriguing observations are essentially unknown.

NO is also a free radical messenger that at physiological concentrations binds to mitochondrial respiratory enzyme complex IV (MRC-IV) to donate single electrons to the oxygen molecule and promote the release of superoxide anion (O_2^-) (Cleeter et al., 1994). NO may additionally be converted to a number of reactive nitrogen species, including *S*-nitrosothiols, to inhibit MRC-I (Brown and Borutaite, 2004), leading to production of O_2^- (Borutaite and Brown, 2006). Moreover, NO increases O_2^- levels by down-regulating mitochondrial uncoupling protein-2 (UCP-2) (Merial et a l., 2000), a member of the mitochondrial anion carrier family that dissipates the proton gradient in the inner mitochondrial membrane, leading to a decrease in ROS production (Korshunov et al., 1997; Andrews et al., 2005). Under normal conditions, the mitochondrion-derived O_2^- is rapidly degraded by superoxide dismutases (SODs) to hydrogen peroxide, which is subsequently converted to water by catalase and glutathione peroxidase. However, under pathological conditions such as hypertension, when the antioxidant defense machinery is defective (Kishi et al., 2004; Tai et al., 2005), NO may cause an accumulation of O_2^- by inhibiting mitochondrial respiratory enzyme activity and down-regulating UCP-2. O_2^- in the RVLM in turn evokes pressor response via activation of sympathetic vasomotor activity (Kimura et al., 2005a; Chan et al., 2006).

We demonstrated previously (Chan et al., 2006) that the molecular synthesis and enzyme activity of mitochondrial manganese SOD (SOD2) are reduced in the RVLM of spontaneously hypertensive rats (SHR). It follows that an interaction between NO and O_2^- in the RVLM, using MRC as the cellular target, may contribute to the unsustained depressor and rebound hypertensive effects after eNOS gene transduction in SHR. This hypothesis was validated in the present study using adenoviral vectors to overexpress eNOS (AdeNOS) and/or SOD2 (AdSOD2) in the RVLM of SHR or normotensive Wistar-Kyoto (WKY) rats.

Materials and Methods

All experimental procedures were carried out in compliance with the guidelines of our institutional animal care committee and were in accordance with the Guide for the Care and Use of Laboratory Animals as adopted and promulgated by the U.S. National Institutes of Health.

Animals. Male adult (10–12-week-old) SHR (215–240 g, $n = 336$) or WKY rats (210–245 g, $n = 286$), purchased from the Experimental Animal Center of the National Applied Research Laboratories, Taiwan, were used. They were housed in an animal room under temperature control (24 ± 0.5°C) and 12-h light-dark (8:00 AM–8:00 PM) cycle. Standard laboratory rat chow (PMI Nutrition International, Brentwood, MO) and tap water were available ad libitum. All animals were allowed to acclimatize for at least 7 days before experimental manipulations.

Construction and Purification of Adenovirus Vectors. Adenoviral vectors encoding *eNOS* or *SOD2* gene were constructed and purified as detailed previously (Tai et al., 2005; Chan et al., 2006). Based on 4,6-diamidino-2-phenylindole staining of adenoviral construct carrying green fluorescence protein (GFP), 80 to 90% of cultured GH_3 neuronal cells were infected with minimal toxicity at a concentration of 100 multiplicity of infection (Supplemental Fig. S1). In addition, the efficacy of AdeNOS to enhance NO production or AdSOD2 to inhibit O_2^- accumulation has been demonstrated (Tai et al., 2005).

In Vivo Gene Transduction of eNOS and/or SOD2 in the RVLM. For in vivo gene delivery, bilateral microinjection of AdeNOS or AdSOD2, adenoviral vectors encoding βgal (Adβgal), or green fluorescence protein (AdGFP) (Tai et al., 2005; Chan et al., 2006) was carried out stereotaxically and sequentially into the RVLM of SHR or WKY rats that were anesthetized with sodium pentobarbital (50 mg/kg i.p.). An adenoviral suspension containing 0.5×10^9 plaque-forming units (pfu)/50 nl was delivered to each injection site over 10 to 15 min using a glass micropipette. For cotransduction, a mixture of AdeNOS and AdSOD2 containing 1×10^9 pfu/50 nl was administered. A total of eight injections (four on each side) were made at two rostrocaudal levels at stereotaxic coordinates of 4.5 or 5 mm posterior to lambda, 1.8 to 2.1 mm lateral to the midline, and 8.0 to 8.5 mm below the dorsal surface of cerebellum. These coordinates cover the confines of RVLM within which sympathetic premotor neurons reside (Ross et al., 1984). The wound was closed in layers, and animals were allowed to recover in individual cages with free access to food and water.

Microinjection of Test Agents into the RVLM. Various pharmacological agents were used to establish a causal role for MRC, NO, and O_2^- in the cellular events and cardiovascular phenotypes induced by gene transduction with AdeNOS and/or AdSOD2 in the RVLM. Bilateral microinjection of test agents was carried out stereotaxically and sequentially into the RVLM, using a glass micropipette and at an injection volume of 50 nl (Tai et al., 2005; Chan et al., 2006, 2007a,b). The stereotaxic coordinates of RVLM used were 4.6 to 4.8 mm posterior to lambda, 1.8 to 2.1 mm lateral to the midline, and 8.0 to 8.5 mm below the dorsal surface of cerebellum. Test agents employed included the MRC-I inhibitor rotenone (Sigma-Aldrich, St. Louis, MO); a mobile mitochondrial electron carrier, coenzyme Q_{10} (CoQ_{10}; Sigma-Aldrich); a nonselective NOS inhibitor, N^{ω}-nitro-L-arginine-methyl ester (L-NAME, Sigma-Aldrich); a potent eNOS inhibitor, N^5-(1-iminoethyl)-L-ornithine (L-NIO; Tocris Cookson, Bristol, UK); an active peroxynitrite decomposition catalyst, 5,10,15,20-tetrakis-(*N*-methyl-4′-pyridyl)-porphyrinato iron (III) (FeTMPyP; Calbiochem, San Diego, CA); a NADPH oxidase inhibitor, apocynin (Calbiochem); or a peroxisome proliferator-activated receptor γ activator, rosiglitazone (Cayman Chemical, Ann Arbor, MI). Microinjection of artificial cerebrospinal fluid (aCSF) or dimethyl sulfoxide served as the vehicle and volume control. The composition of aCSF was 117 mM NaCl, 25 mM $NaHCO_3$, 11 mM glucose, 4.7 mM KCl, 2.5 mM $CaCl_2$, 1.2 mM $MgCl_2$, and 1.2 mM NaH_2PO_4. The doses used were established in pilot studies or were the same as in our previous studies (Tai et al., 2005; Chan et al., 2001, 2005a, 2006), in which individual test agent was used for the same purpose as in the present study.

Measurement of Systemic Arterial Pressure and Heart Rate. Changes in cardiovascular parameters were evaluated after gene transduction of eNOS and/or SOD2 into the RVLM. Mean systemic arterial pressure (MSAP) and heart rate (HR) were recorded in conscious rats using a radiotelemetry system (UA-10; Data Sciences International, Minneapolis, MN) (Chan et al., 2007b). Under sodium pentobarbital (50 mg/kg i.p.) anesthesia, a flexible catheter attached to a telemetry transmitter was inserted into the rat abdominal aorta just below the renal arteries. The catheter was secured in place with tissue glue, and the transmitter was attached to the abdominal muscle and remained in the abdominal cavity for the duration of the experiment. The skin was closed using nonabsorbable suture (3-0). Rats were allowed to recover from surgery for 3 days in individual cages positioned over an RLA-3000 radiotelem-

etry receiver before gene transduction. The MSAP and HR were recorded continuously for 30 min every day between 13:00 and 15:00, and telemetry data were collected for a maximum of 49 days. In a separate series of experiments, the short-term effect of rotenone, CoQ_{10}, or apocynin on MSAP or HR was determined on day 14 or 28 after gene transduction in animals that were maintained under propofol anesthesia (30 mg/kg/h i.v.).

Collection of Tissue Samples from Ventrolateral Medulla. To correlate biochemical changes in the RVLM with cardiovascular phenotypes after gene transduction, we routinely collected ventrolateral medullary tissues at various intervals after microinjection of AdeNOS and/or AdSOD2 into the RVLM. Rats were killed with an overdose of sodium pentobarbital (100 mg/kg i.p.) and perfused intracardially with 150 ml of warm (37°C) saline containing heparin (100 U/ml). The brain was rapidly removed and placed on dry ice, blocked in the coronal plane, and sectioned at 300-μm thickness in a cryostat. Both sides of the ventrolateral medulla covering the RVLM were collected by micropunches made with a stainless steel bore (1 mm i.d.) (Chan et al., 2005a, 2006, 2007a; Tai et al., 2005). Medullary tissues collected from animals under anesthesia but without treatment served as the basal control.

Isolation of Mitochondrial Fractions. To investigate whether MRC is the cellular target for NO and $O_2^{\cdot-}$ interaction after gene transduction of eNOS and/or SOD2 in the RVLM or to measure UCP-2 expression, mitochondria were isolated from the ventrolateral medulla by discontinuous Percoll gradient centrifugation according to procedures described previously (Chan et al., 2005b, 2007a). This procedure, which was performed at 4°C and completed within 2 h after tissue collection, yields 10 to 15% of the total mitochondria and enriches the mitochondrial fraction by at least 10-fold compared with tissue homogenates (Kantrow et al., 1997). The purity of the mitochondrial-rich fraction was verified by the expression of MRC-IV (Naithani et al., 2003). Total protein in the mitochondrial or cytosolic extracts was estimated by the method of Bradford with a protein assay kit (Bio-Rad Laboratories, Hercules, CA).

Assays For Activity of Mitochondrial Respiratory Enzymes. Activities of MRC were measured immediately after mitochondrial isolation, according to procedures reported previously (Wu et al., 2007) and using a thermostatically regulated ThermoSpectronic spectrophotometer (Fisher Scientific UK, Loughborough, UK). At least duplicate determination was carried out for each tissue sample in all enzyme activity assays, and the activity was expressed in nmol/mg protein/min. For NADH cytochrome *c* reductase (NCCR; marker for coupling capacity between complexes I and III) activity, the mitochondrial fraction (20 μg of protein) was incubated in a mixture containing 50 mM K_2HPO_4 buffer, pH 7.4, 1.5 mM KCN, 1 mM β-NADH, and 20 μM rotenone at 37°C for 2 min.

After the addition of 0.1 mM cytochrome *c*, the reduction of oxidized cytochrome *c* was measured as the difference in the presence or absence of rotenone at 550 nm for 3 min at 37°C. The molar extinction coefficient of cytochrome *c* at 550 nm is 18,500 M/cm.

Determination of succinate cytochrome *c* reductase (SCCR; marker for coupling capacity between complexes II and III) activity in the mitochondrial fraction (30 μg) was performed in 40 mM K_2HPO_4 buffer, pH 7.4, and 1.5 mM KCN, supplemented with 20 mM succinate. After a 5-min equilibration at 37°C, 50 μM cytochrome *c* was added, and the reaction was monitored at 550 nm for 3 min at 37°C.

The cytochrome *c* oxidase (CCO, marker enzyme for MRC-IV) activity was measured by oxidation of the reduced cytochrome *c*. The activity is defined as the first-order rate constant and is calculated from known concentration of ferrocytochrome *c* and the enzyme amount in the assay mixture. Mitochondrial fraction (30 μg) and 500 mM K_2HPO_4, pH 7.4, was preincubated at 30°C for 5 min. A 45 μM ferrocytochrome *c* was added to start the reaction monitored at 550 nm for 3min at 30°C. The background rate was measured after the addition of 1.0 μM $K_3Fe(CN)_6$.

Measurement of ATP Concentration. We measured tissue levels of ATP to decipher whether AdeNOS- and/or AdSOD2-induced changes in $O_2^{\cdot-}$ levels and cardiovascular responses are consequential to bioenergetic failure. Samples collected from ventrolateral medulla of rats that received the same experimental manipulations were pooled and homogenized in a protein extraction solution (Pierce, Rockford, IL). The supernatant after centrifugation at 10,000*g* for 10 min was subject to determination of ATP concentration, using an ATP bioluminescence assay (Roche Diagnostics, Mannheim, Germany) (Wu et al., 2007). Light emitted from a luciferase-mediated reaction and measured by a tube luminometer (Berthold Detection Systems, Pforzheim, Germany) was used to calculate the measured values.

Measurement of $O_2^{\cdot-}$ by Lucigenin-Enhanced Chemiluminescence. $O_2^{\cdot-}$ production was determined by lucigenin-enhanced chemiluminescence according to previously described and validated methods (Chan et al., 2005a, 2006; Tai et al., 2005). $O_2^{\cdot-}$ production was calculated and expressed in micromoles per minute per milligram of protein. Specificity for $O_2^{\cdot-}$ was determined by adding SOD (350 U/ml) to the incubation medium.

Western Blot Analysis. Western blot analysis of total protein extracted from ventrolateral medulla was carried out as detailed previously (Tai et al., 2005; Chan et al., 2006) using a mouse monoclonal antiserum against nitrotyrosine (1:1000; Calbiochem), a rabbit polyclonal antiserum against UCP-2 (1:2000; Calbiochem), α-tubulin (1:5000; Sigma), or a mitochondrial inner membrane marker, prohibitin (1:1000; NeoMarkers, Fremont, CA). This was followed by incubation with horseradish peroxidase-conjugated goat anti-rabbit IgG (Jackson Immunoresearch Laboratories, West Grove, PA) or sheep anti-mouse IgG (GE Healthcare, Chalfont St. Giles, Buckinghamshire, UK). Specific antibody-antigen complex was detected using an enhanced chemiluminescence Western Blot detection system (PerkinElmer Life Sciences, Waltham, MA). The amount of detected nitrotyrosine was quantified by Photo-Print Plus software (ETS Vilber-Lourmat, Marne La Vallee, France) and was expressed as the ratio to α-tubulin protein.

Isolation of RNA and Reverse Transcription Real-Time Polymerase Chain Reaction. A fundamental premise in the present study is that delivery of the transgenes to the RVLM effectively induced the targeted gene products. To detect copper/zinc SOD1, SOD2, extracellular SOD3, nNOS, iNOS, or eNOS mRNA expression, total RNA from samples of ventrolateral medulla was isolated with TRIzol reagent (Invitrogen, Carlsbad, CA) according to the manufacturer's protocol. All RNA isolated was quantified by spectrophotometry, and the optical density 260/280-nm ratio was determined. Reverse transcription (RT) reaction was performed using a SuperScript Preamplification System (Invitrogen) for the first-strand cDNA synthesis. Real-time polymerase chain reaction (PCR) analysis was performed by amplification of cDNA using a LightCycler instrument (Roche Diagnostics) (Chan et al., 2005a, 2007b). The primers used in real-time PCR amplification (Table 1) were designed using Roche LightCycler probe design software 2.0 based on sequence information from the NCBI database, and were synthesized by Genemed Biotechnologies (San Francisco, CA). PCR reaction for each sample was carried out in duplicate for all the cDNA and for the glyceraldehyde-3-phosphate dehydrogenase control. Fluorescence signals from the amplified products were quantitatively assessed using the LightCycler software program (version 3.5). Second derivative maximum mode was chosen with baseline adjustment set in the arithmetic mode (Chan et al., 2005a, 2007b).

Double Immunofluorescence Staining and Laser Confocal Microscopy. We assessed the distribution of eNOS and SOD2 protein in the RVLM after gene transduction by double immunofluorescence staining. In brief, free-floating 25-μm sections of the medulla oblongata were incubated with a mouse monoclonal antiserum against eNOS (1:1000; BD Biosciences, San Jose, CA), together with a rabbit polyclonal antiserum against SOD2 (1:1000; StressGene, Victoria, BC, Canada). The sections were subsequently incubated

concurrently with a goat anti-mouse IgG conjugated with Alexa Fluor 564 (Invitrogen) for eNOS and a goat anti-rabbit IgG conjugated with Alexa Fluor 488 (Invitrogen) for SOD2. Viewed under a Fluorview FV300 laser scanning confocal microscope (Olympus, Tokyo, Japan), immunoreactivity for eNOS exhibited red fluorescence, and that for SOD2 exhibited green fluorescence. The occurrence of yellow fluorescence on merged images indicated coexpression of eNOS and SOD transgenes.

Histology. With the exception of animals used for biochemical or molecular analyses, the brain stem was removed from animals after they were killed by an overdose of sodium pentobarbital (100 mg/kg i.v.), and fixed in 30% sucrose in 10% formaldehyde-saline solution for ≥72 h. Frozen 25-μm sections of the medulla oblongata were stained with 1% Neural red for histological verification of the location of microinjection sites. The expression of GFP in the medulla oblongata was detected by confocal microscopy.

TABLE 1
Primers used in real-time PCR analysis

Gene	GenBank Accession #	Forward Primer	Reverse Primer	Amplicon Size
				bp
SOD1	NM_017050	CACTCTAAGAAACATGGCG	CTGAGAGTGAGATCACACG	124
SOD2	NM_017051	TTCAGCCTGCACTGAAG	GTCACGCTTGATAGCCTC	122
SOD3	NM_012880	CTTGACCTGGTTGAGAAGATAG	GATCTGTGGCTGATCGG	153
eNOS	NM_021838	TTCCGCTACCAGCCTGAC	TCACCGTGCCCATGAGT	124
nNOS	U67309	CCCACAGTCTGGTTGCT	CGTCGCCCGATGACTTTC	102
iNOS	U03699	TGGAGGTGCTGGAAGAGTT	GGAGGAGCTGATGGAGTAGT	101
GAPDH	NM_008084	TCCATGACAACTTTGGCATTG	TCACGCCACAGCTTTCCA	103

bp, base pair(s).

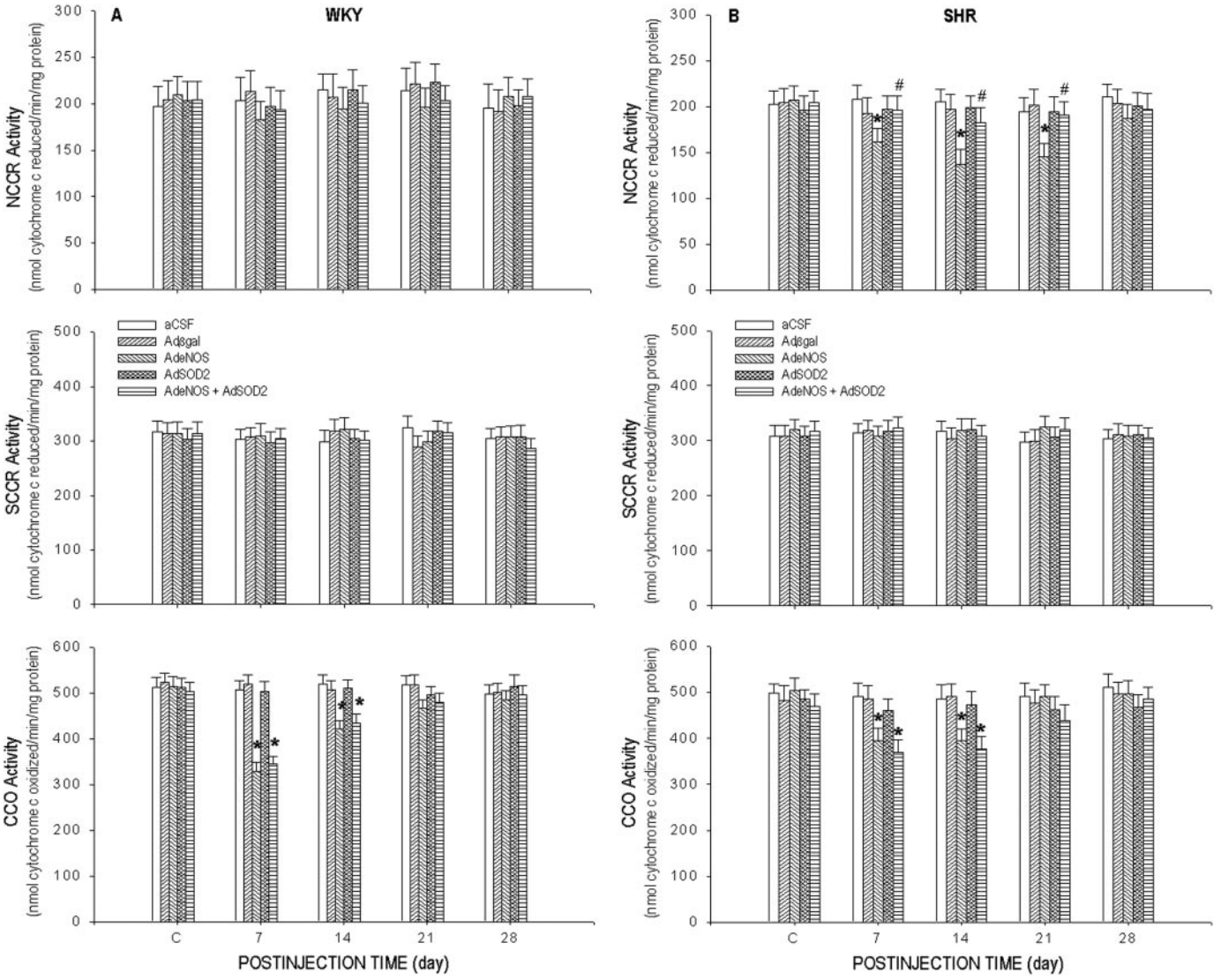

Fig. 1. Time course changes in mitochondrial NCCR, SCCR, or CCO activity in ventrolateral medulla of WKY rats (A) or SHR (B) that received bilateral microinjection into the RVLM of aCSF, Adβgal, AdeNOS, AdSOD2, or AdeNOS+AdSOD2. Values are mean ± S.E., n = 4–5 animals in each group. ∗, $p < 0.05$ versus corresponding aCSF group; #, $p < 0.05$ versus corresponding AdeNOS group in the Scheffé multiple-range test.

Statistical Analysis. All values are expressed as mean ± S.E. One- or two-way analysis of variance with repeated measures was used to assess group means, as appropriate, to be followed by the Scheffé multiple-range test for post hoc assessment of individual means. A value of $p < 0.05$ was taken to indicate statistical significance.

Results

Effects of Gene Transduction of eNOS and/or SOD2 in RVLM on Mitochondrial Respiratory Enzyme Activity and ATP Content in Ventrolateral Medulla. Our first series of experiments determined whether WKY rats or SHR exhibited differential bioenergetic responses to gene transduction of eNOS or SOD2 in the RVLM. Microinjection of AdeNOS to the RVLM of WKY rats, alone or together with AdSOD2, inhibited CCO activity but not NCCR or SCCR activity in ventrolateral medulla when determined on day 7 or 14 after injection (Fig. 1A). On the other hand, NCCR activity was depressed 7, 14, or 21 days after transduction of eNOS in the RVLM of SHR, and CCO activity was reduced on days 7 or 14 (Fig. 1B). The suppression of NCCR, but not CCO, activity by the *eNOS* transgene was significantly reversed on cotransduction with AdSOD2. Microinjection of AdSOD2 alone, on the other hand, did not exert discernible effect on the activity of those mitochondrial respiratory enzymes in SHR or WKY rats. On day 14 after eNOS gene transduction, the decrease of NCCR or CCO activity in SHR was significantly reversed in a dose-related manner by bilateral microinjection into the RVLM of an eNOS inhibitor, L-NIO (10, 50, or 100 pmol) (Fig. 2A). Given at an equimolar concentration, the nonselective NOS inhibitor L-NAME (100 pmol) promoted comparable antagonism on the reduced NCCR (80 ± 5 versus 74 ± 6%, $n = 5$) or CCO (74 ± 4 versus 70 ± 6%, $n = 5$) activity after eNOS gene transduction. Microinjection of the peroxynitrite decomposition catalyst FeTMPyP (10 or 50 pmol), on the other hand, attenuated only the reduction in NCCR, but not CCO, activity (Fig. 2B). The reduction in CCO activity on day 14 after AdeNOS transfection in WKY rats was also prevented by L-NAME or L-NIO but not by FeTMPyP (data not shown).

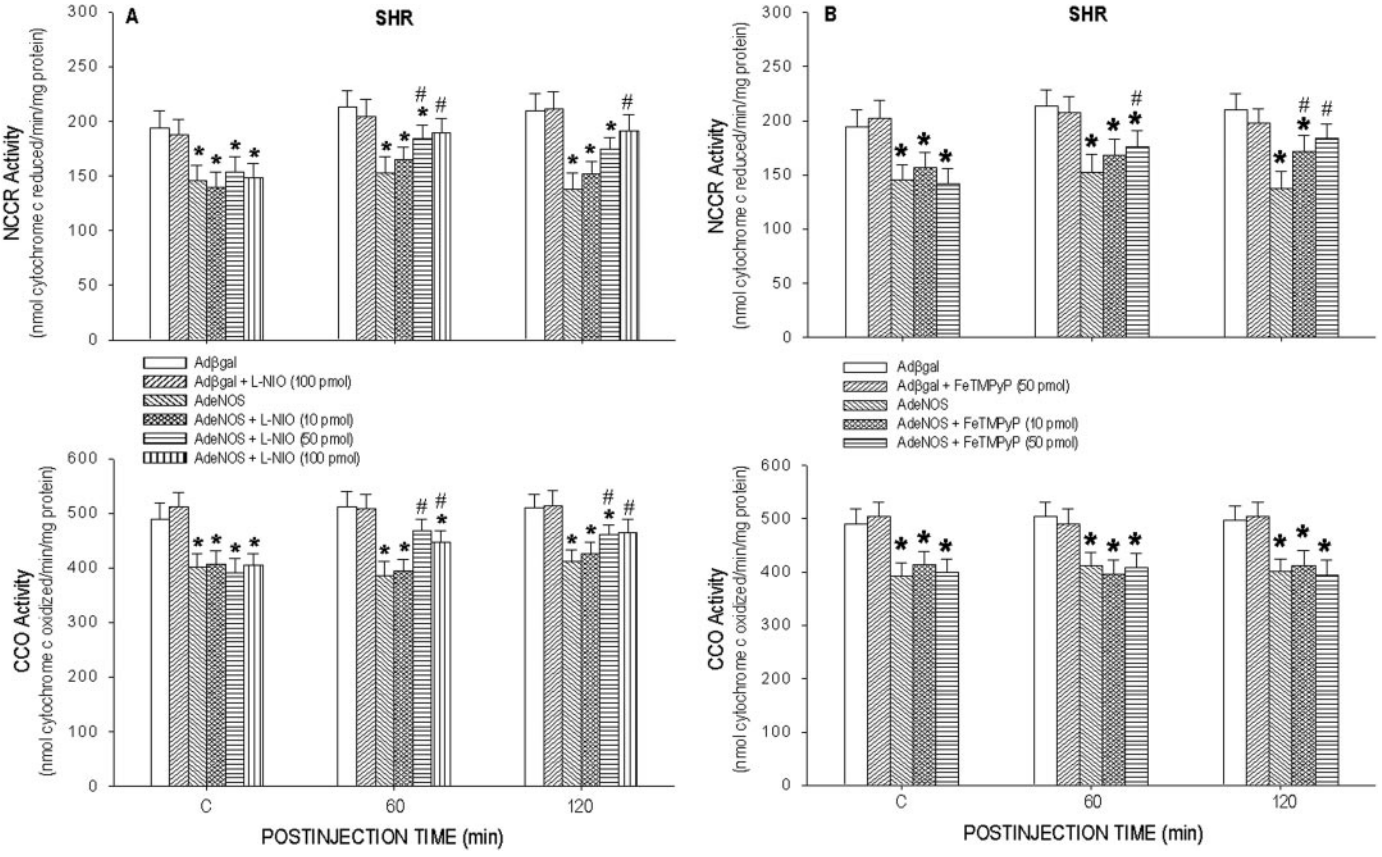

Fig. 2. Mitochondrial NCCR or CCO activity in ventrolateral medulla of SHR that received bilateral microinjection into the RVLM of L-NIO (A) or FeTMPyP (B) on day 14 after gene transduction of Adβgal or AdeNOS in the RVLM. For clarity, data on Adβgal+L-NAME are not shown because they essentially duplicated those of Adβgal+L-NIO. Values are mean ± S.E., $n = 4$–5 animals in each group. *, $p < 0.05$ versus corresponding Adβgal group; #, $p < 0.05$ versus corresponding AdeNOS group in the Scheffé multiple-range test.

TABLE 2

Cellular ATP content in ventrolateral medulla after microinjection bilaterally into the RVLM of aCSF, Adβgal, AdeNOS, and/or AdSOD2

Values are mean ± S.E. of samples pooled from four to five animals in each experiment. No significant difference in two-way analysis of variance.

	aCSF	Adβgal	AdeNOS	AdSOD2	AdeNOS/AdSOD2
			pmol/mg protein		
Control	62.3 ± 3.6	59.6 ± 3.4	63.1 ± 4.3	60.7 ± 3.8	59.9 ± 3.2
Day 14	58.7 ± 4.1	60.8 ± 4.5	60.5 ± 3.8	62.1 ± 3.3	60.7 ± 4.6
Day 21	60.1 ± 3.8	61.7 ± 3.9	59.7 ± 4.2	61.3 ± 4.3	58.4 ± 3.5

Compared with aCSF control, bilateral microinjection of AdeNOS and/or AdSOD2 into the RVLM of SHR or WKY rats induced minimal alterations of ATP content in ventrolateral medulla, detected on day 14 or 21 after gene transduction (Table 2). Control injection of Adβgal was also minimally effective.

Temporal Effects of Gene Transduction of eNOS and/or SOD2 in RVLM on Superoxide Levels in Ventrolateral Medulla. Our second series of experiments examined whether gene transduction of eNOS or SOD2 also elicited disparate effects on the differential levels of O_2^- in the RVLM of the two strains of rats. As observed in our previous studies (Tai et al., 2005; Chan et al., 2006), the basal level of O_2^- in ventrolateral medulla was higher in SHR than WKY rats. Measured on day 14 or 21 after gene delivery of AdeNOS, there were further increases of this O_2^- level in SHR, whereas AdSOD2 elicited a decrease (Fig. 3). On the other hand, neither transgene affected the O_2^- level in ventrolateral medulla of WKY rats. The AdeNOS-induced increase in O_2^- level in the SHR was significantly attenuated by cotransduction of AdSOD2 (Fig. 3). Similar response was also observed in the SHR after bilateral microinjection into the RVLM of the nonselective NOS inhibitor L-NAME (100 pmol) or a selective eNOS inhibitor, L-NIO (100 pmol) (Fig. 4A). The tissue level of O_2^- in the RVLM of SHR, but not WKY rats (data not shown), was also elevated on day 28 or 35 after eNOS transduction (Fig. 4B). Microinjected into the bilateral RVLM of a mobile mitochondrial electron carrier on day 28 or 35 after the gene transduction of eNOS, CoQ_{10} (2.5 nmol), but not the NADPH oxidase inhibitor apocynin (2.5 nmol), significantly attenuated the induced accumulation of O_2^- level in the RVLM of SHR. Treatment with L-NIO (0.43 $\pm$ 0.12 μmol/min/mg protein, $n = 5$), L-NAME (0.35 $\pm$ 0.09 μmol/min/mg protein, $n = 5$), CoQ_{10} (0.35 $\pm$ 0.11 μmol/min/mg protein, $n = 5$), or apocynin (0.41 $\pm$ 0.09 μmol/min/mg protein, $n = 5$) exerted no discernible effect on O_2^- level in the RVLM of WKY (0.36 $\pm$ 0.13 μmol/min/mg protein, $n = 6$), which was not altered on day 28 after gene delivery of AdeNOS (compare Figure 3A).

Temporal Effects of Gene Transduction of eNOS in RVLM on Peroxynitrite Production in Ventrolateral Medulla. The observation that the peroxynitrite decomposition catalyst FeTMPyP blunted the AdeNOS-induced reduction in mitochondrial NCCR activity and the augmentation in O_2^- level effected by the transgene suggest that the eNOS-derived NO may interact with O_2^- to form peroxynitrite in the

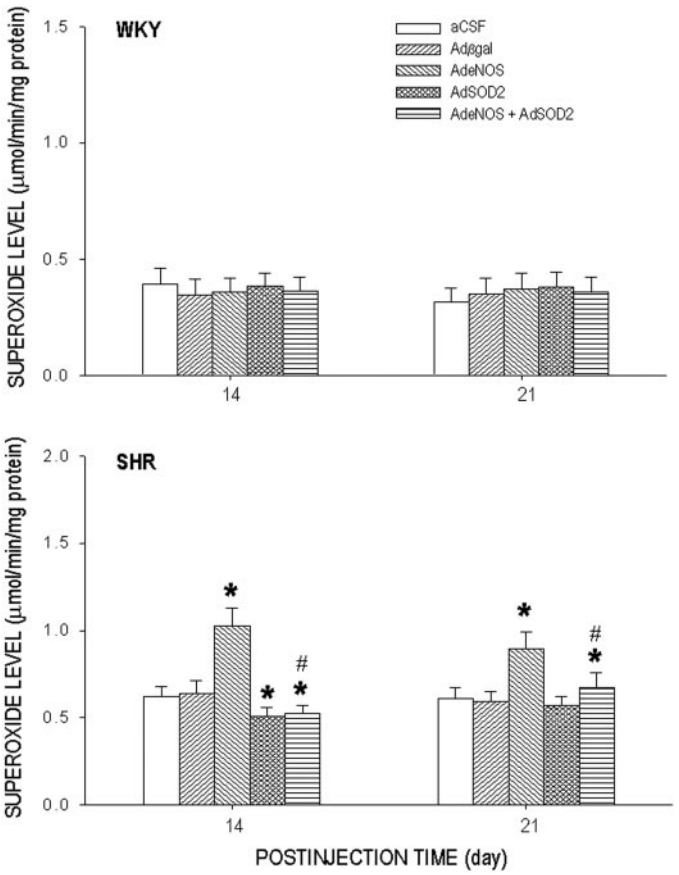

Fig. 3. Superoxide level in ventrolateral medulla of SHR or WKY rats detected on day 14 or 21 after bilateral microinjection into the RVLM of aCSF, Adβgal, AdeNOS, AdSOD2, or AdeNOS+AdSOD2. Values are mean $\pm$ S.E., $n = 4$–5 animals in each group. *, $p < 0.05$ versus corresponding aCSF or Adβgal group; #, $p < 0.05$ versus corresponding AdeNOS group in the Scheffé multiple-range test.

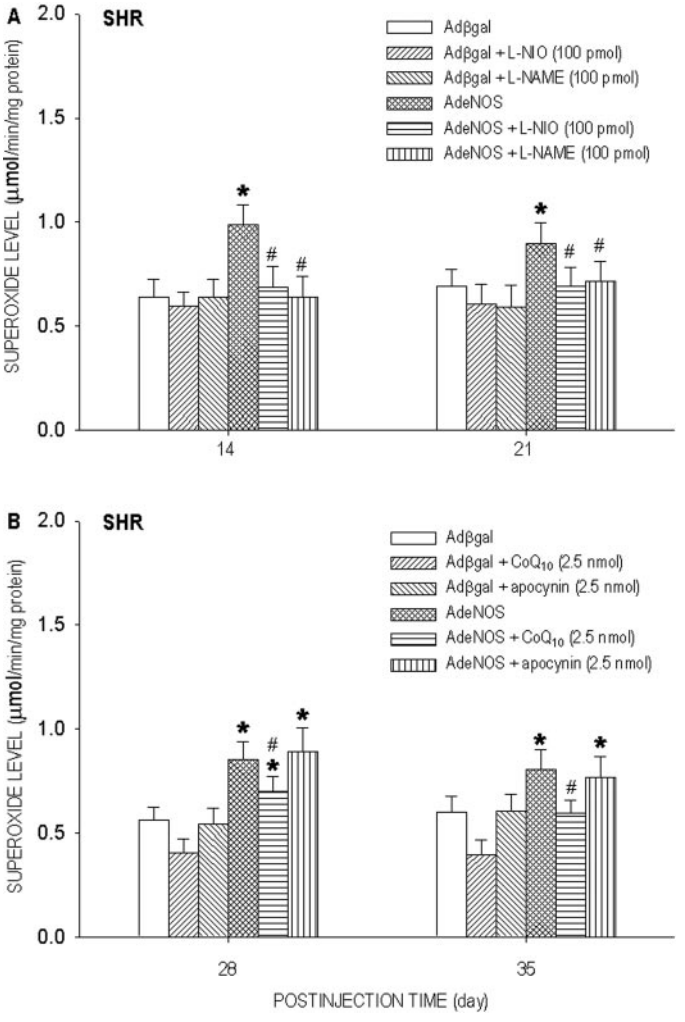

Fig. 4. Superoxide level in ventrolateral medulla of SHR that received bilateral microinjection into the RVLM of L-NIO or L-NAME on day 14 or 21 (A) or CoQ_{10} or apocynin (APO) day 28 or 35 (B) after gene transduction of Adβgal or AdeNOS in the RVLM. Values are mean $\pm$ S.E. of quadruplicate analyses on samples pooled from five to six animals in each group. *, $p < 0.05$ versus Adβgal group; #, $p < 0.05$ versus AdeNOS group in the Scheffé multiple-range analysis.

RVLM of SHR. Our third series of experiments evaluated this possibility. Compared with WKY rats, the expression of 3-nitrotyrosine, an experimental index of peroxynitrite (Reiter et al., 2000), in ventrolateral medulla was significantly increased 7, 14, or 21 days after gene transduction of eNOS in the RVLM of SHR (Fig. 5A). Measured on day 14 or 21, the AdeNOS-induced increase in 3-nitrotyrosine in SHR was significantly attenuated by cotransduction of AdSOD2 (Fig. 5B).

Temporal Effects of Gene Transduction of eNOS or SOD2 in RVLM on MSAP and HR. The cardiovascular effects of manipulations of NO and O_2^- level in the RVLM by gene transduction were investigated in our fourth series of experiments. Consistent with our previous report (Tai et al., 2005), application of AdeNOS (0.5×10^9 pfu) to the RVLM promoted a significant decrease in MSAP or HR in SHR or WKY rats that lasted 14 days after gene transduction (Fig. 6). The AdeNOS-induced hypotension in SHR was followed by a rebound hypertension that became significant between days 28 and 35 after injection. Transduction of AdSOD2 (0.5×10^9 pfu) resulted in significant hypotension and bradycardia in SHR, but not WKY rats, that lasted 11 days. Comicroinjection of AdeNOS and AdSOD2 (final titer, 0.5×10^9 pfu) into the bilateral RVLM significantly augmented the amplitude and prolonged the duration (21 days) of the induced hypotension and bradycardia in SHR but not WKY rats. In particular, the maximal decrease in MSAP after cotransduction of AdeNOS and AdSOD2 (59.6 ± 2.9 mm Hg, $n = 10$) was significantly greater than the mathematical sum of that promoted individually by AdeNOS (31.5 ± 2.3 mm Hg, $n = 10$) or AdSOD2 (15.1 ± 2.4 mm Hg, $n = 10$). Furthermore, the rebound hypertension observed in AdeNOS-treated SHR was absent on delivery of AdeNOS and AdSOD2. Transduction of Adβgal, on the other hand, had no discernible effect on MSAP or HR in either strain of rat. Cotransduction of AdeNOS and AdSOD2 to regions adjacent to the confine of RVLM (e.g., lateral reticular nucleus, ventromedial medulla, areas lateral to the nucleus ambiguus) also did not affect the baseline MSAP or HR in SHR or WKY rats (data not shown).

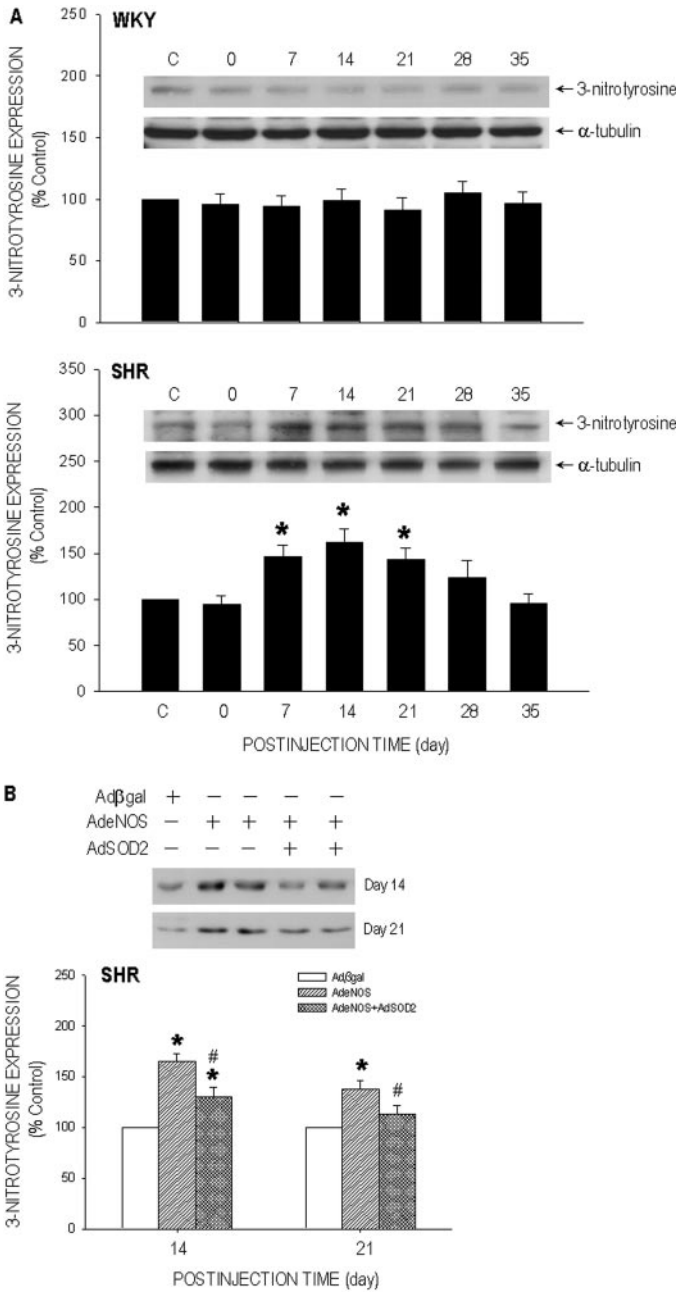

Fig. 5. Time course changes in nitrotyrosine expression in ventrolateral medulla of WKY rats or SHR (A) that received bilateral microinjection into the RVLM of AdeNOS, or 3-nitrotyrosine or α-tubulin expressions in ventrolateral medulla of SHR on day 14 or 21 (B) after gene transduction of Adβgal, AdeNOS or AdSOD2+AdSOD2 in the RVLM. Expression of α-tubulin was included as a loading control. Values are mean ± S.E., n = 4–5 animals in each group. *, $p < 0.05$ versus corresponding basal expression (C) in the Scheffé multiple-range test.

Effect of Mitochondrial Respiratory Complex I on Depressor Response to Gene Transduction of eNOS in RVLM of WKY Rats. Results from our first four series of experiments suggest that depression of MRC-I activity and increase in O_2^- production in the RVLM are associated with an antagonism of the vasodepressor effect of the eNOS transgene in the RVLM of SHR. Our fifth series of experiments was performed to ascertain that such a relationship is causal with the use of a loss-of-function approach by depressing the activity of MRC-I in the RVLM of normotensive WKY rats, which was not affected by eNOS transgene (Fig. 1A). On day 14 after AdeNOS transduction in the RVLM of WKY rats, bilateral microinjection of the MRC-I inhibitor rotenone (500 pmol) into the RVLM significantly reversed the depressor and bradycardic responses induced by the *eNOS* transgene during the 120-min observation period (Fig. 7). Rotenone (500 pmol) also evoked a pressor response in WKY rats that received Adβgal gene transduction. The rotenone-evoked pressor response was significantly reversed by bilateral comicroinjection into the RVLM of the SOD mimetic tempol (50 nmol; +9.6 ± 1.7 versus +2.1 ± 1.1 mm Hg, $n = 5$), in the Adβgal-transduced WKY rats. In a separate series of experiments, bilateral microinjection into the RVLM of rotenone resulted in a significant increase in tissue level of O_2^- (rotenone, +76 ± 6%, $n = 5$) in ventrolateral medulla of WKY rats on day 14 after eNOS gene transduction.

Effect of NADPH Oxidase Inhibitor or Protection of the Mitochondrial Respiratory Enzyme Activity on Rebound Hypertension after eNOS Gene Transduction in RVLM of SHR. Our sixth series of experiments further deciphered the contribution of O_2^- generated by the MRC or NADPH oxidase to the rebound hypertension after eNOS gene transduction in the SHR. On day 28 (Fig. 8) or 35 (data not shown) after AdeNOS gene transduction in SHR, micro-

injection of a mobile mitochondrial electron carrier CoQ_{10}, (5 nmol), but not the NADPH oxidase inhibitor apocynin (5 nmol), into the bilateral RVLM significantly alleviated the rebound hypertension during the 120-min observation period. No rebound hypertension in WKY (123.6 ± 3.8 mm Hg, $n = 5$) rats was detected on day 28 after eNOS gene transduction; CoQ_{10} (118.3 ± 4.5 mm Hg, $n = 5$) or apocynin (121.6 ± 3.9 mm Hg, $n = 5$) treatment also did not significantly affect MSAP. At the end of a 120-min observation period, the tissue level of O_2^- in ventrolateral medulla of AdeNOS-transduced SHR was significantly lower in CoQ_{10}-treated rats (0.66 ± 0.12 μmol/min/mg protein, $n = 5$) than apocynin-treated (0.92 ± 0.15 μmol/min/mg protein, $n = 5$).

Temporal Effects of eNOS Gene Transduction in RVLM on Mitochondrial UCP-2 Expression in Ventrolateral Medulla. The observation that rebound hypertension after gene transduction in the RVLM of SHR occurred after waning of eNOS expression prompted us to search for the mechanism that underlies this lag period. One possibility is that NO may suppress mitochondrial UCP-2 (Merial et al., 2000), leading to elevated tissue levels of O_2^- that elicited rebound hypertension. Our seventh series of experiments evaluated this possibility. Bilateral microinjection into the RVLM of AdeNOS significantly decreased UCP-2 protein expression in the mitochondrial fraction of samples from ventrolateral medulla of SHR or WKY rats (Fig. 9). Such a down-regulation of mitochondrial UCP-2 expression became significantly different from sham control on day 7, 14, or 21 after gene transduction of eNOS in the RVLM and was not affected by cotransduction of AdSOD2 into the RVLM of SHR or WKY rats.

Effect of Transcriptional Up-Regulation of UCP in the RVLM on the Elevated Superoxide Levels in Ventrolateral Medulla after Gene Transduction of eNOS in SHR. Our eighth series of experiments further established a causal role for UCP down-regulation and the induced increase in O_2^- level in the ventrolateral medulla. On day 21 or 28 after eNOS gene transduction in the RVLM of SHR, the increase in tissue level of O_2^- in ventrolateral medulla was reversed in a dose-related manner by bilateral microinjection into the RVLM of rosiglitazone (1 or 5 nmol), an activator of the peroxisome proliferator-activated receptor that acts as a transcriptional factor for UCP-2 induction (Nolte et al., 1998), delivered 24 h before measurement of O_2^- (Fig. 10). The O_2^- level in ventrolateral medulla of WKY rats, which was not altered after eNOS gene transduction (0.40 ± 0.12 μmol/min/mg protein, $n = 6$), was not affected by rosiglitazone (5 nmol).

Temporal Expression of eNOS or SOD2 mRNA in Ventrolateral Medulla after Microinjection of AdeNOS and/or AdSOD2 into RVLM. A fundamental premise in the present study is that delivery of the transgenes to the RVLM effectively induced the targeted gene products. Our ninth series of experiments ascertained this premise. Consistent with our previous findings on protein expression (Tai et al., 2005; Chan et al., 2006), real-time RT-PCR analysis revealed that, given individually (Fig. 11) or together (data not shown), bilateral microinjection into the RVLM of AdeNOS and/or AdSOD2 resulted in significant and comparable up-regulation of eNOS and SOD2 mRNA expression in ventrolateral medulla of SHR or WKY rats that lasted, respectively, 14 or 11 days. In contrast, there were no parallel changes in nNOS, iNOS, SOD1, or SOD3 mRNA (data not shown). Microinjection of Adβgal also did not affect basal eNOS or SOD2 mRNA expression in the RVLM (Fig. 11).

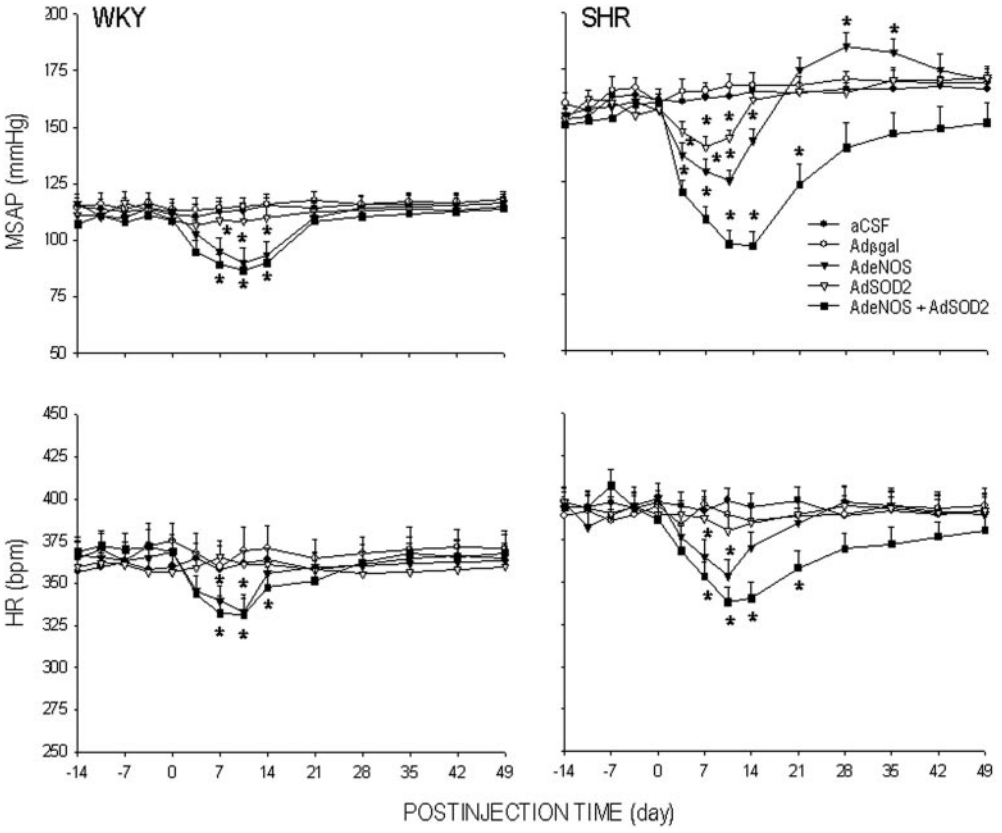

Fig. 6. Time course changes in mean systemic arterial pressure (MSAP) or heart rate (HR) in SHR or WKY rats that received bilateral microinjection into the RVLM of aCSF, Adβgal, AdeNOS, AdSOD2 or AdeNOS+AdSOD2. Values are mean ± S.E., $n = 5–6$ animals in each group. $*p < 0.05$ versus aCSF or Adβgal group at corresponding time-points in the Scheffé multiple-range test.

Cellular Expression of eNOS and SOD2 after Microinjection of AdeNOS and AdSOD2 into RVLM. Another critical issue is that gene delivery is effective at the cellular level and is restricted to the RVLM. Our final series of experiments addressed this issue. Figure 12, A and B, showed the presence of eNOS or SOD2 immunoreactivity in RVLM cells of SHR 11 days after cotransduction of AdeNOS and AdSOD2 in this medullary site. It is noteworthy that against the clearly defined nucleus, eNOS or SOD2 expression was confined to the cytoplasm. Furthermore, merged images (Fig. 12C) demonstrated that all eNOS-positive cells in the RVLM were immunoreactive to SOD2. Based on the manifestation of green fluorescence from GFP, Fig. 12D illustrates that microinjection of AdGFP resulted in a distribution that was restricted to the anatomical confines of the RVLM. Similar results were observed in WKY rats that received cotransduction of AdeNOS and AdSOD2 in the RVLM (data not shown).

Discussion

Overexpression of NO in the RVLM by eNOS gene transduction was proposed for treatment of neurogenic hypertension (Zanzinger, 1999) because NO deficiency in the RVLM contributes to the neural mechanisms of hypertension in SHR (Kagiyama et al., 1998; Chan et al., 2003; Tandai-Hiruma et al., 2005). The *eNOS* transgene, however, fails to provide sustained depressor effect (Kishi et al., 2002; Tai et al., 2005) and is followed by rebound hypertension (Tai et al., 2005). The present study presented novel observations to suggest that an interaction between NO and O_2^- in the RVLM, using MRC-I in the mitochondrial respiratory chain as the cellular target via formation of peroxynitrite, contributes to those cardiovascular outcomes after eNOS gene transduction in SHR.

Our results indicate that MRC-I is the main target for the interaction between NO and O_2^- in the RVLM during neurogenic hypertension. We found that gene transduction of AdeNOS in SHR, but not WKY rats, significantly inhibited MRC-I activity, as indicated by a suppression of NCCR (marker for coupling capacity between complexes I and III), but not SCCR (marker for coupling capacity between complexes II and III) activity. The observations that L-NIO or L-NAME reversed the inhibition of NCCR activity by AdeNOS indicated that those cellular processes are dependent on eNOS-derived NO production. The manifestation of comparable degree of antagonism by equimolar concentration of L-NIO or L-NAME further imply minimal contributions from nNOS- and iNOS-derived NO to the inhibition of NCCR or CCO activity after eNOS gene transduction. We also found that microinjection of AdeNOS into the RVLM selectively up-regulated eNOS, but not nNOS or iNOS mRNA. These

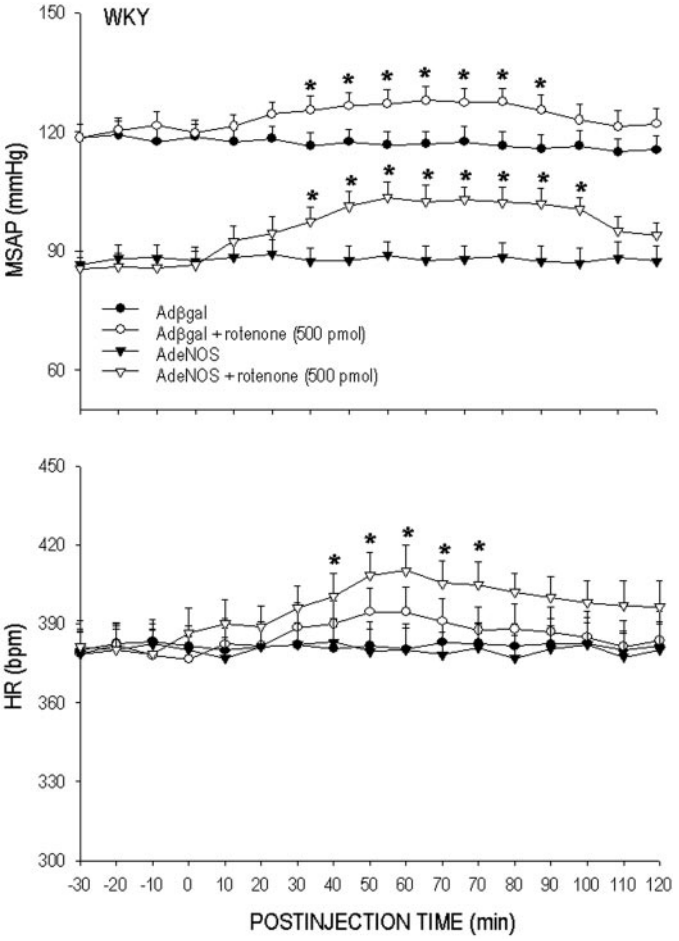

Fig. 7. Time course changes in MSAP and HR in anesthetized WKY rats that received bilateral microinjection into the RVLM of rotenone on day 14 after gene transduction of Adβgal or AdeNOS in the RVLM. Values are mean ± S.E., $n = 5–6$ animals in each group. $*p < 0.05$ versus Adβgal or AdeNOS group at corresponding time-points in the Scheffé multiple-range test.

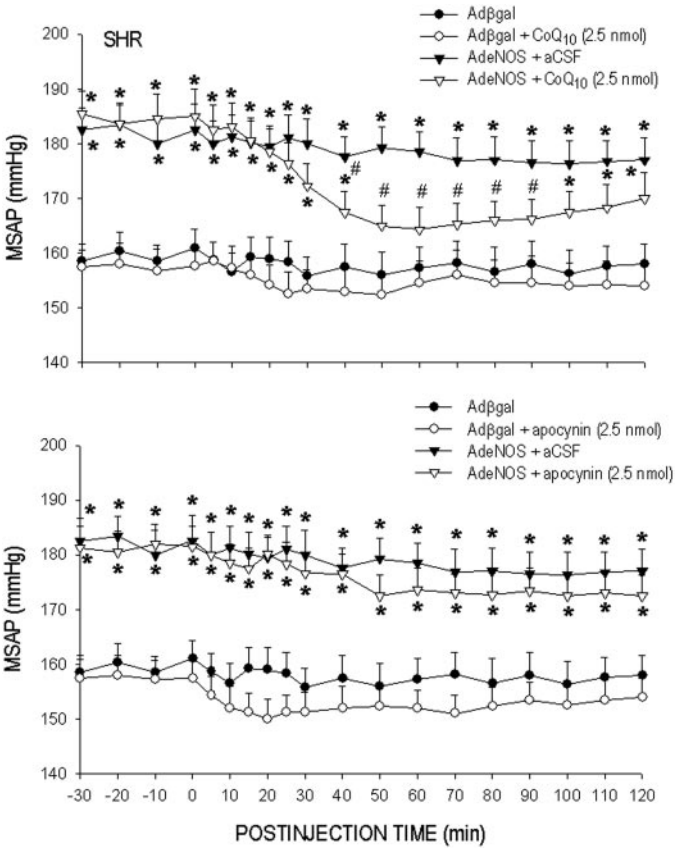

Fig. 8. Time course changes in MSAP in anesthetized SHR that received bilateral microinjection of CoQ_{10} or apocynin (APO) into the RVLM on day 28 after gene transduction with Adβgal or AdeNOS in the RVLM. Values are mean ± S.E., $n = 6–7$ animals in each group. *, $p < 0.05$ versus Adβgal group; #, $p < 0.05$ versus AdeNOS group in the Scheffé multiple-range analysis.

results are consistent with previous reports on protein expression of the NOS isoforms after eNOS gene transduction (Kishi et al., 2002, 2003; Tai et al., 2005).

It is noteworthy that the suppression of MRC-I activity in the RVLM of SHR after eNOS gene transduction was also significantly prevented in the short term by a peroxynitrite decomposition catalyst or in the long term by cotransduction of AdSOD2. We reported previously (Chan et al., 2006) that a reduction in protein expression and enzyme activity of SOD2 underlies the augmented basal level of O_2^- in the RVLM of SHR. Furthermore, MRC-I is a main source of mitochondrial O_2^- (Kudin et al., 2004) and is selectively sensitive to peroxynitrite (Murray et al., 2003). It is thus conceivable that a reaction between the augmented NO production and the enhanced tissue level of O_2^- after gene transduction of eNOS leads to the formation of peroxynitrite in the RVLM, which when coupled with SOD2 deficiency (Chan et al., 2006) results in suppression of MRC-I activity in ventrolateral medulla of SHR. The temporal increase in expression of nitrotyrosine, the product of peroxynitrite-meditated nitration of tyrosine residue (Reiter et al., 2000), in the ventrolateral medulla of AdeNOS-treated SHR that paralleled those of enhanced tissue level of O_2^- or depression of MRC-1 activity, but not WKY rats, provides further credence to this notion. Moreover, it is also likely that an action of peroxynitrite on MRC-1 in the RVLM of SHR may also contribute to the sustained augmentation of O_2^- level in the RVLM of SHR after AdeNOS transduction.

Our results also indicate that MRC-IV is another target for eNOS transgene in the RVLM. Transfection of eNOS depressed CCO (marker enzyme for MRC-IV) activity in the RVLM of both SHR and WKY rats, an action that was antagonized by L-NAME or L-NIO, but not FeTMPyP or cotransfected AdSOD2. This suggests that eNOS-derived NO exerts a direct depressant effect on MRC-IV activity. In this regard, NO binds to the Fe^{2+} center of cytochrome α_3 and the $Cu^{2+}B$ center of CCO to elicit a reversible inhibition on MRC-IV activity (Stevens et al., 1979; Mason et al., 2006). It is intriguing that despite the induced MRC-IV inhibition by the *eNOS* transgene there was only minimal alteration in O_2^- level in ventrolateral medulla of WKY rats. This observation implies the presence of an effective mitochondrial SOD2 system in the RVLM of WKY rats for degradation of the accumulated O_2^- after gene transduction. Alternatively, it suggests that MRC-IV plays a minor role in mitochondrial O_2^- formation and that MRC-I is the major O_2^--producing sites in brain mitochondria (Kudin et al., 2004).

Mitochondrial dysfunction is associated with the pathogenesis of several cardiovascular disorders, including hypertension (Kimura et al., 2005b; Callera et al., 2006). Together with our previous findings (Chan et al., 2006), we propose that there are at least two mechanisms via which mitochon-

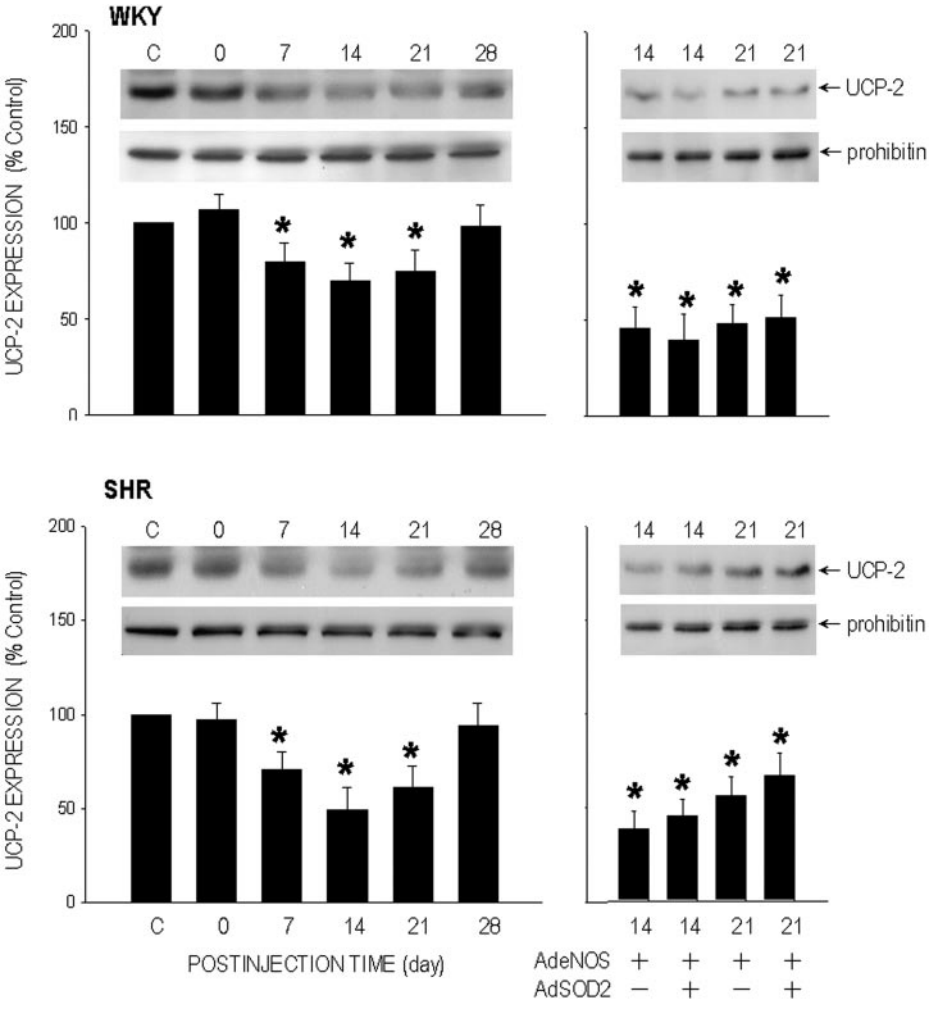

Fig. 9. Time course changes of UCP-2 expression in the mitochondrial fraction of samples of ventrolateral medulla from WKY rats or SHR that received bilateral microinjection into the RVLM of AdeNOS (left), or UCP-2 expression in ventrolateral medulla of WKY rats or SHR on day 14 or 21 after gene transduction with AdeNOS or AdeNOS +AdSOD2 in the RVLM (right). Expression of the mitochondrial inner membrane protein prohibitin was included as a loading control. Values are mean ± S.E., $n = 5–6$ animals in each group. *, $p < 0.05$ versus sham control (C) in the Scheffé multiple-range test.

drial dysfunction in the RVLM of SHR may contribute to neurogenic hypertension. The first mechanism involves a reduction in protein expression and enzyme activity of mitochondrial SOD2 in the RVLM (Chan et al., 2006), resulting in accumulation of O_2^- that induces sympathetic overexcitation and pressor effect (Kishi et al., 2002; Kimura et al., 2005a; Chan et al., 2006). Mitochondria isolated from *sod2*-null mice exhibit higher levels of mitochondrial O_2^- than the wild type, of which is attenuated by a SOD mimetic (Morten et al., 2006). The present results further showed that gene transduction of SOD2 to the RVLM resulted in depressor responses in SHR. The second mechanism engages counteraction of the sympathoinhibitory and depressor effect of NO (Zanzinger et al., 1995; Zanzinger, 1999) by mitochondria-derived O_2^- in the RVLM. We observed that cotransduction of AdSOD2 in the RVLM of SHR augmented both the magnitude and duration of hypotensive response induced by overexpression of eNOS, together with a significant reversal of AdeNOS-induced O_2^- production to levels that are comparable with those in WKY rats. Moreover, the MRC-I inhibitor attenuated the depressor response to eNOS overexpression in the RVLM of normotensive WKY rats. It is noteworthy that all these cellular events and hemodynamic changes occurred with minimal alteration in cellular ATP contents. As such, it is unlikely that the AdeNOS- and/or AdSOD2-induced changes in O_2^- levels and cardiovascular responses are consequential to bioenergetic failure.

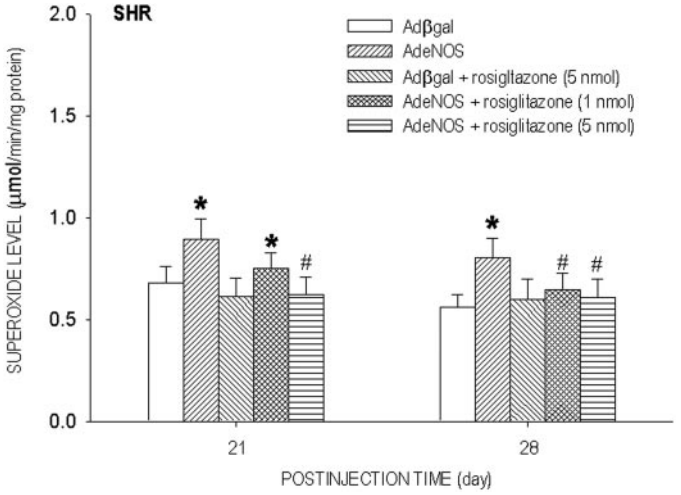

Fig. 10. Superoxide level in ventrolateral medulla of SHR detected on day 21 or 28 after bilateral microinjection into the RVLM of Adβgal or AdeNOS, or with additional rosiglitazone treatment, delivered to the RVLM 24 h before superoxide measurement. Values are mean ± S.E., $n = 5–6$ animals in each group. *, $p < 0.05$ versus corresponding Adβgal group; #, $p < 0.05$ versus corresponding AdeNOS group in the Scheffé multiple-range test. Data on Adβgal- and AdeNOS-transduced groups are adapted from Fig. 4.

Enhancement of NO production by gene transduction of eNOS to the RVLM (Kishi et al., 2004) has been demonstrated to promote sympathoinhibitory and depressor responses in hypertensive rats (Kishi et al., 2002; Tai et al., 2005), although the normalized arterial pressure is followed by rebound hypertension. We reported previously (Tai et al., 2005) that this rebound phenomenon is attributed to O_2^- generation. The present study extends this finding to reveal that CoQ_{10}, a mobile mitochondrial electron carrier, but not apocynin, a NADPH oxidase inhibitor, significantly reversed the augmented O_2^- level in the RVLM, alongside a suppression of rebound hypertension seen after eNOS gene transduction. These observations suggest that cellular O_2^- generated by the mitochondrial MRC, but not NADPH oxidase, is responsible for the AdeNOS-promoted re-

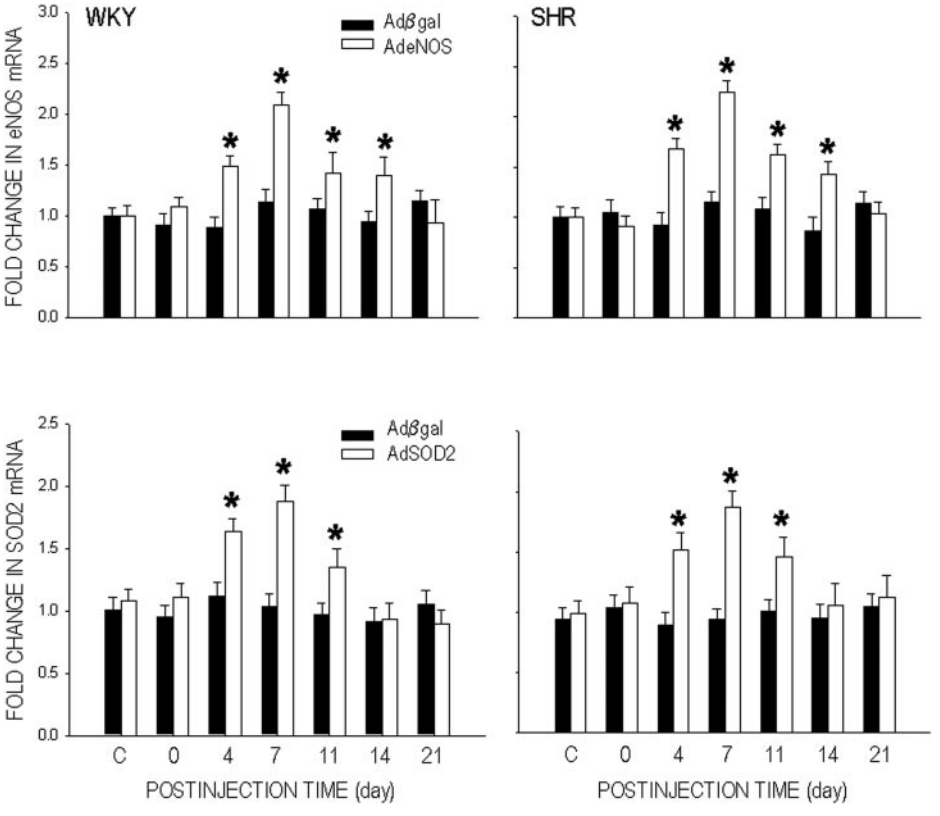

Fig. 11. Real-time PCR results showing -fold changes in eNOS or SOD2 mRNA expression detected from the ventrolateral medulla of SHR or WKY rats at day 4, 7, 11, 14, or 21 after bilateral microinjection into the RVLM (day 0) of AdeNOS+AdSOD2. Values are mean ± S.E. of quadruplicate analyses on samples pooled from five to six animals in each group. *, $P < 0.05$ versus basal control (C) group in the Scheffé multiple-range analysis.

bound hypertension. We noted a trend of reduction in tissue O_2^- level in the RVLM by CoQ_{10} in animals treated with Adβgal. These findings pointed to a crucial engagement of mitochondrial electron transport chain in tonic regulation of cellular ROS homeostasis.

We recognize that the up-regulated eNOS mRNA expression in ventrolateral medulla has returned to baseline 21 days after AdeNOS gene transduction, the time point at which rebound hypertension began. One candidate that we identified to link transduction of AdeNOS gene with this rebound hypertension is mitochondrial UCP-2, which diminishes mitochondrial O_2^- production (Nègre-Salvayre et al., 1997). We found a closely correlated temporal sequence of up-regulation of eNOS mRNA or protein expression (Tai et al., 2005), down-regulation of mitochondrial UCP-2 or elevated O_2^- production in ventrolateral medulla, and manifestation of rebound hypertension after AdeNOS transduction in the RVLM of SHR. A causal role for UCP-2 down-regulation in the augmentation of O_2^- production was established when transcriptional up-regulation of UCP-2 with the peroxisome proliferator-activated receptor γ activator rosiglitazone abrogated the elevated O_2^- during which rebound hypertension took place. It is intriguing to note that whereas mitochondrial UCP-2 was down-regulated in the ventrolateral medulla of SHR and WKY rats after the eNOS gene transduction, elevated tissue level of O_2^- and rebound hypertension were only observed in SHR. Given the abundance of SOD2 in the mitochondria of WKY rats, we reasoned that the increased production of O_2^- because of the AdeNOS-induced UCP-2 down-regulation may be rapidly dismutated. This antioxidant defense mechanism, on the other hand, was significantly reduced in the mitochondria of SHR (Chan et al., 2006), allowing oxidative injury to go unchecked and persisted over time after AdeNOS gene transduction. Our results showed that comparable inhibition of UCP-2 expression was exhibited in ventrolateral medulla of SHR or WKY rats that received AdeNOS alone or in combination with AdSOD2. These results suggest the possibility of a direction inhibitory action of NO on UCP-2 expression that is independent of O_2^-. The underlying molecular pathway remains to be established. UCP-2 belongs to the mitochondrial anion carrier family located in the inner mitochondrial membrane, which dissipates the mitochondrial proton gradient and causes a decrease in ROS production (Korshunov et al., 1997; Andrews et al., 2005). Our results therefore suggest that NO generated by the eNOS transgene while it was still prevalent down-regulated UCP-2 expression, leading to the subsequent increase in mitochondrial O_2^- level in the RVLM that underlies the rebound hypertension in SHR.

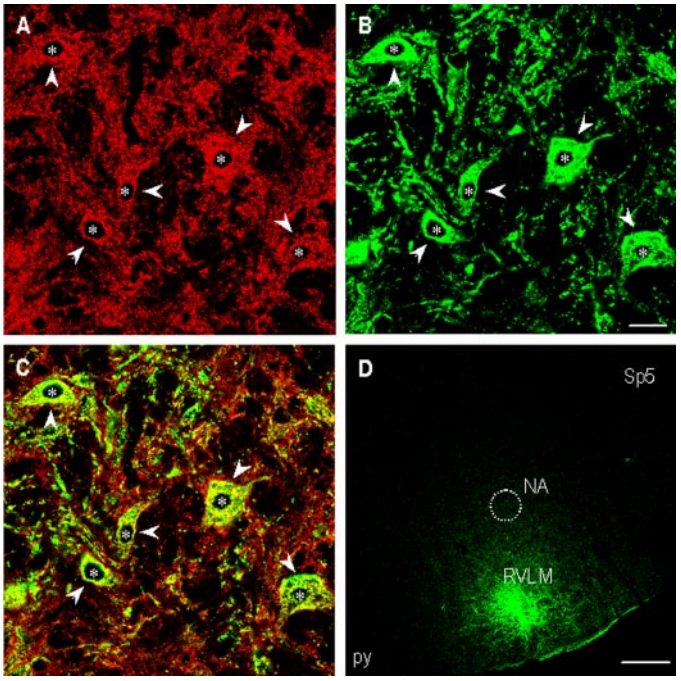

Fig. 12. Representative laser scanning confocal microscopic images showing the presence of eNOS (white arrowheads; A) or SOD2 (white arrowheads; B) immunoreactivity in RVLM cells on day 11 after bilateral comicroinjection into the RVLM of AdeNOS and AdSOD2. Merged image (white arrowheads; C) illustrates colocalization of eNOS and SOD2 immunoreactivity in RVLM cells. Also shown is the distribution of green fluorescence protein (GFP; D) in the RVLM 11 days after microinjection of AdGFP into the RVLM. *, the nucleus. Scale bar, 200 μm in A–C; 20 μm in D. NA, nucleus ambiguus; Sp5, spinal trigeminal nucleus; py, pyramidal tract.

The reason for NO-dependent cardiovascular effects to outlast the expression of individual mRNA after gene transduction of eNOS and SOD2 are not immediately clear. Oxidative stress has been shown to cause a deficiency in tetrahydrobiopterin (BH_4), an essential cofactor for eNOS, in blood vessels (Landmesser et al., 2003). Conversely, reducing O_2^- generation enhances BH_4 levels and prompts endogenous eNOS to regain its normal function to produce NO (Antoniades et al., 2006; Li et al., 2006). We also recognize that apart from the mitochondrial MRC, eNOS may produce O_2^- at the expense of NO through a process referred to as "eNOS uncoupling" (Xia et al., 1998). Whether this mechanism is involved in the generation of O_2^- and its contribution to cardiovascular effects after eNOS gene transduction, however, awaits further investigation. One hint arises from *eNOS* transgenic mice (eNOS-Tg) and double transgenic mice (*eNOS*/*GCH*-Tg) that included both eNOS and cyclohydrolase 1 (GCH), the rate-limiting enzyme in BH_4 biosynthesis (Bendall et al., 2005). Whereas NO production is markedly increased in the aorta of both strains of transgenic mice compared with wild-type littermates (Adlam et al., 2007), the magnitude of augmented NO level is comparable in eNOS/GCH-Tg and eNOS-Tg mice. This suggests that eNOS uncoupling after overexpression of eNOS is minimal.

We recognize that a fundamental premise in the present study is that the delivered transgenes effectively transduced the targeted gene products in the RVLM. Our results from real-time RT-PCR confirmed that coadministration of AdeNOS or AdSOD2 into the RVLM elicited an up-regulation of eNOS or SOD2 mRNA in ventrolateral medulla that exhibited a temporal profile that was comparable with the induced eNOS or SOD2 protein expression (Kishi et al., 2002, 2003; Kimura et al., 2005; Tai et al., 2005; Chan et al., 2006). Double immunofluorescence staining coupled with confocal microscopy further established that application of AdeNOS and AdSOD2 leads to cotransduction of eNOS and SOD2 within the cytoplasm of RVLM cells. Our results also refuted the possibility that the unsustained depressor response after overexpression eNOS in RVLM of SHR was a consequence of reduced transduction efficiency. Both SHR and WKY rats exhibited comparable time course and amplitude of up-regulation of eNOS or SOD2 in ventrolateral medulla on cotransduction of AdeNOS and AdSOD2.

Three factors determined our choice of eNOS gene transduction to increase NO production in the RVLM. First, transduction of adenoviral vectors encoding *eNOS* in brain tissue has been demonstrated to exert minimal inflammatory and neurotoxic effects while eliciting a 2-fold increase in NO levels (Kishi et al., 2002, 2003). Second, eNOS is reported to be more useful in discriminating de novo production from endogenous production than nNOS in the RVLM (Kishi et al., 2002, 2003). Third, contrary to an augmented nNOS (Edwards et al., 2004) or a reduced iNOS (Chan et al., 2001) mRNA level in SHR, eNOS transcription in the RVLM is comparable between SHR and WKY rats (Kishi et al., 2002; Tai et al., 2005). Transduction of eNOS gene would thus minimize the potential confounding influence of difference in transcriptional regulation of the transduced gene between SHR and WKY rats. We are aware that overexpression of *eNOS* increases systemic blood flow (Brevetti et al., 2003). The contribution of differential blood flow induced in the RVLM to our observed differential hypotensive effects of eNOS transgene in SHR and WKY awaits further elucidation. The possibility that the differential cardiovascular responses to eNOS gene transduction between SHR and WKY rats is due to differential membrane injury because of oxidative stress as a result of enhanced and O_2^- in the RVLM of SHR is deemed unlikely. The amount of thiobarbituric acid-reactive substances, an experimental index for lipid peroxidation by free radicals, in stroke-prone SHR rats that received eNOS gene transduction in the RVLM is not different from those that received Adβgal (Kishi et al., 2003).

In conclusion, based on differential results obtained from transduction of AdeNOS and/or AdSOD2 in the RVLM of SHR or WKY rats, the present study revealed that an interaction between NO and O_2^- that targets MRC-I in the RVLM via the formation of peroxynitrite contributes to the unsustained depressor response after overexpression eNOS in SHR. Prophylactic or therapeutic potential against neurogenic hypertension is implicated for an enhancement of NO production by up-regulating eNOS expression in the RVLM. Nevertheless, our results from gene transduction also prompted a precautionary note; there is a potential detrimental consequence for eNOS-generated NO in the RVLM in an environment of pre-existing oxidative stress. A recent study (Waki et al., 2006) demonstrated the contribution of eNOS-generated NO in the nucleus tractus solitarii to hypertension in SHR. This demonstration, together with results from our present study, raises the issues of whether simple up-regulation of eNOS expression by gene transduction is a reasonable strategic target for the prevention or therapy of neurogenic hypertension. On the other hand, the possibility that regulation of mitochondrial functions may be amenable to manipulation opens a new vista for the development of remedial strategies against neurogenic hypertension.

Acknowledgments

This work was carried out during the tenure of S.H.H.C. as the National Chair Professor of Neuroscience appointed by the Ministry of Education, and Sun Yat-sen Research Chair Professor appointed by the National Sun Yat-sen University, Taiwan, Republic of China.

References

Adlam D, Bendall JK, De Bono JP, Alp NJ, Khoo J, Nicoli T, Yokoyama M, Kawashima S, and Channon KM (2007) Relationships between nitric oxide-mediated endothelial function, eNOS coupling and blood pressure revealed by eNOS-GTP cyclohydrolase 1 double transgenic mice. *Exp Physiol* **92:**119–126.

Andrews ZB, Diano S, and Horvath TL (2005) Mitochondrial uncoupling proteins in the CNS: in support of function and survival. *Nat Rev Neurosci* **6:**829–840.

Antoniades C, Shirodaria C, Warrick N, Cai S, de Bono J, Lee J, Leeson P, Neubauer S, Ratnatunga C, Pillai R, et al. (2006) 5-methyltetrahydrofolate rapidly improves endothelial function and decrease superoxide production in human vessels. Effects on vascular tetrahyrobiopterin availability and endothelial nitric oxide synthase coupling. *Circulation* **114:**1193–1201.

Bendall JK, Alp NJ, Warrick N, Cai S, Adlam D, Rockett K, Yokoyama M, Kawashima S, and Channon KM (2005) Stoichiometric relationships between endothelial tetrahydrobiopterin, eNOS activity and eNOS coupling in vivo: insights from transgenic mice with endothelial-targeted GTP cyclohydrolase 1 and eNOS over-expression. *Circ Res* **97:**864–871.

Borutaite V and Brown GC (2006) *S*-nitrosothiol inhibition of mitochondrial complex I causes a reversible increase in mitochondrial hydrogen peroxide production. *Biochim Biophys Acta* **1757:**562–566.

Brevetti LS, Chang DS, Tang GL, Sarkar R, and Messina LM (2003) Overexpression of endothelial nitric oxide synthase increases skeletal muscle blood flow and oxygenation in severe rat hind limb ischemia. *J Vasc Surg* **38:**820–826.

Brown GC and Borutaite V (2004) Inhibition of mitochondrial respiratory complex I by nitric oxide, peroxynitrite and S-nitrosothiols. *Biochim Biophys Acta* **1658:**44–49.

Callera GE, Tostes RC, Yogi A, Montezano AC, and Touyz RM (2006) Endothelin-1-induced oxidative stress in DOCA-salt hypertension involves NADPH-oxidase-independent mechanisms. *Clin Sci* **110:**243–253.

Chan JY, Chang AY, Wang LL, Ou CC, and Chan SH (2007a) Protein kinase C-dependent mitochondrial translocation of proapoptotic protein Bax on activation of inducible nitric oxide synthase in rostral ventrolateral medulla mediates cardiovascular depression during experimental endotoxemia. *Mol Pharmacol* **71:**1129–1139.

Chan JY, Wang LL, Chao YM, and Chan SH (2003) Down-regulation of basal iNOS at rostral ventrolateral medulla is innate in SHR. *Hypertension* **41:**563–570.

Chan SH, Hsu KS, Huang CC, Wang LL, Ou CC, and Chan JY (2005a) NADPH oxidase-derived superoxide anion mediates angiotensin II-induced pressor effect via activation of p38 mitogen-activated protein kinase in the rostral ventrolateral medulla. *Circ Res* **97:**772–780.

Chan SH, Tai MH, Li CY, and Chan JY (2006) Reduction in molecular synthesis or enzyme activity of superoxide dismutases and catalase contributes to oxidative stress and neurogenic hypertension in spontaneously hypertensive rats. *Free Radic Biol Med* **40:**2028–2039.

Chan SH, Wang LL, Tseng HL, and Chan JY (2007b) Upregulation of AT_1 receptor gene on activation of protein kinase Cβ/nicotinamide adenine dinucleotide diphosphate oxidase/ERK1/2/c-*fos* signaling cascade mediates long-term pressor effect of angiotensin II in rostral ventrolateral medulla. *J Hypertens* **25:**1845–1861.

Chan SH, Wang LL, Wang SH, and Chan JY (2001) Differential cardiovascular responses to blockade of nNOS or iNOS in rostral ventrolateral medulla of the rat. *Br J Pharmacol* **133:**606–614.

Chan SH, Wu KL, Wang LL, and Chan JY (2005b) Nitric oxide- and superoxide-dependent mitochondrial signaling in endotoxin-induced apoptosis in the rostral ventrolateral medulla of rats. *Free Radic Biol Med* **39:**603–618.

Cleeter MW, Cooper JM, Darley-Usmar VM, Moncada S, and Schapira AH (1994) Reversible inhibition of cytochrome c oxidase, the terminal enzyme of the mitochondrial respiratory chain, by nitric oxide. Implications for neurodegenerative diseases. *FEBS Lett* **345:**50–54.

Dampney RAL (1994) Functional organization of central pathways regulating the cardiovascular system. *Physiol Rev* **74:**323–364.

Edwards MA, Loxley RA, Powers-Martin K, Lipski J, McKitrick DJ, Arnolda LF, and Phillips JK (2004) Unique levels of expression of *N*-methyl-D-aspartate receptor subunits and neuronal nitric oxide synthase in the rostral ventrolateral medulla of the spontaneously hypertensive rat. *Brain Res Mol Brain Res* **129:**33–43.

Kagiyama S, Tsuchihashi T, Abe I, and Fujishima M (1998) Enhanced depressor response to nitric oxide in the rostral ventrolateral medulla of spontaneously hypertensive rats. *Hypertension* **31:**1030–1034.

Kantrow SP, Taylor DE, Carraway MS, and Piantadosi CA (1997) Oxidative metabolism in rat hepatocytes and mitochondria during sepsis. *Arch Biochem Biophys* **345:**278–288.

Kimura Y, Hirooka Y, Sagara Y, Ito K, Kishi T, Shimokawa H, Takeshita A, and Sunagawa K (2005a) Overexpression of inducible nitric oxide synthase in rostral ventrolateral medulla causes hypertension and sympathoexcitation via an increase in oxidative stress. *Circ Res* **96:**252–260.

Kimura S, Zhang GX, Nishiyama A, Shokoji T, Yao L, Fan YY, Rahman M, and Abe Y (2005b) Mitochondria-derived reactive oxygen species and vascular MAP kinases: comparison of angiotensin II and diazoxide. *Hypertension* **45:**438–444.

Kishi T, Hirooka Y, Ito K, Sakai K, Shimokawa H, and Takeshita A (2002) Cardiovascular effects of overexpression of endothelial nitric oxide synthase in the rostral ventrolateral medulla in stroke-prone spontaneously hypertensive rats. *Hypertension* **39:**264–268.

Kishi T, Hirooka Y, Kimura Y, Ito K, Shimokawa H, and Takeshita A (2004) Increased reactive oxygen species in rostral ventrolateral medulla contribute to neural mechanisms of hypertension in stroke-prone spontaneously hypertensive rats. *Circulation* **109:**2357–2362.

Kishi T, Hirooka Y, Kimura Y, Sakai K, Ito K, Shimokawa H, and Takeshita A (2003) Overexpression of eNOS in RVLM improves impaired baroreflex control of heart rate in SHRSP. *Hypertension* **41:**255–260.

Korshunov SS, Skulachev VP, and Starkov AA (1997) High protonic potential actuates a mechanism o f production of reactive oxygen species in mitochondria. *FEBS Lett* **416:**15–18.

Kudin AP, Bimpong-Buta NY, Vielhaber S, Elger CE, and Kunz WS (2004) Charac-

terization of superoxide-producing sites in isolated brain mitochondria. *J Biol Chem* **279:**4127–4135.
Landmesser U, Dikalov S, Price SR, McCann L, Fukai T, Holland SM, Mitch WE, and Harrison DG (2003) Oxidation of tetrahydrobiopterin leads to uncoupling of endothelial cell nitric oxide synthase in hypertension. *J Clin Invest* **111:**1201–1209.
Li H, Witte K, August M, Brausch I, Gödtel-Armbrust U, Habermeier A, Closs EI, Oelze M, Münzel T, and Förstermann U (2006) Reversal of endothelial nitric oxide synthase uncoupling and up-regulation of endothelial nitric oxide synthase expression lowers blood pressure in hypertensive rats. *J Am Coll Cardiol* **47:**2536–2544.
Mason MG, Nicholls P, Wilson MT, and Cooper CE (2006) Nitric oxide inhibition of respiration involves both competitive (heme) and noncompetitive (copper) binding to cytochrome *c* oxidase. *Proc Natl Acad Sci U S A* **103:**708–713.
Mayorov DN (2005) Selective sensitization by nitric oxide of sympathetic baroreflex in rostral ventrolateral medulla of conscious rabbits. *Hypertension* **45:**901–906.
Merial C, Bouloumie A, Trocheris V, Lafontan M, and Galitzky J (2000) Nitric oxide-dependent downregulation of adipocyte UCP-2 expression by tumor necrosis factor-α. *Am J Physiol Cell Physiol* **279:**C1100–C1106.
Morten KJ, Ackrell BA, and Melov S (2006) Mitochondrial reactive oxygen species in mice lacking superoxide dismutase 2. Attenuation via antioxidant treatment. *J Biol Chem* **281:**3354–3359.
Murray J, Taylor SW, Zhang B, Ghosh SS, and Capaldi RA (2003) Oxidative damage to mitochondrial complex I due to peroxynitrite: identification of reactive tyrosines by mass spectrometry. *J Biol Chem* **278:**37223–37230.
Naithani S, Saracco SA, Butler CA, and Fox TD (2003) Interactions among COX1, COX2, and COX3 mRNA-specific translational activator proteins on the inner surface of the mitochondrial inner membrane of Saccharomyces cerevisiae. *Mol Biol Cell* **14:**324–333.
Nègre-Salvayre A, Hirtz C, Carrera G, Cazenave R, Troly M, Salvayre R, Pénicaud L, and Casteilla L (1997) A role for uncoupling protein-2 as a regulator of mitochondrial hydrogen peroxide generation. *FASEB J* **11:**809–815.
Nolte RT, Wisely GB, Westin S, Cobb JE, Lambert MH, Kurokawa R, Rosenfeld MG, Willson TM, Glass CK, and Milburn MV (1998) Ligand binding and co-activator assembly of the peroxisome proliferator-activated receptor-gamma. *Nature* **395:**137–143.
Reiter CD, Teng RJ, and Beckman JS (2000) Superoxide reacts with nitric oxide to nitrate tyrosine at physiological pH via peroxynitrite. *J Biol Chem* **275:**32460–32466.
Ross CA, Ruggiero DA, Park DH, Joh TH, Sved AF, Fernandez-Pardal J, Saavedra JM, and Reis DJ (1984) Tonic vasomotor control by the rostral ventrolateral medulla: effect of electrical and chemical stimulation of the area containing C1 adrenaline neurons on arterial pressure, heart rate and plasma catecholamine and vasopressin. *J Neurosci* **4:**474–494.
Stevens TH, Brudvig GW, Bocian DF, and Chan SI (1979) Structure of cytochrome a_3-Cu_{a3} couple in cytochrome *c* oxidase as revealed by nitric oxide binding studies. *Proc Natl Acad Sci U S A* **76:**3320–3324.
Tai MH, Wang LL, Wu KL, and Chan JY (2005) Increased superoxide anion in rostral ventrolateral medulla contributes to hypertension in spontaneously hypertensive rats via interactions with nitric oxide. *Free Radic Biol Med* **38:**450–462.
Tandai-Hiruma M, Horiuchi J, Sakamoto H, Kemuriyama T, Hirakawa H, and Nishida Y (2005) Brain neuronal nitric oxide synthase neuron-mediated sympathoinhibition is enhanced in hypertensive Dahl rats. *J Hypertens* **23:**825–834.
Waki H, Murphy D, Yao ST, Kasparov S, and Paton JF (2006) Endothelial NO synthase activity in nucleus tractus solitarii contributes to hypertension in spontaneously hypertensive rats. *Hypertension* **48:**644–650.
Wu KL, Hsu C, and Chan JY (2007) Impairment of the mitochondrial respiratory enzyme activity triggers sequential activation of apoptosis-inducing factor-dependent and caspase-dependent signaling pathways to induce apoptosis after spinal cord injury. *J Neurochem* **101:**1552–1566.
Xia Y, Tsai AL, Berka V, and Zweier JL (1998) Superoxide generation from endothelial nitric oxide synthase. A Ca^{2+}/calmodulin-dependent and tetrahydrobiopterin regulatory process. *J Biol Chem* **273:**25804–25808.
Zanzinger J (1999) Role of nitric oxide in the neural control of cardiovascular function. *Cardiovasc Res* **43:**639–649.
Zanzinger J, Czachurski J, and Seller H (1995) Inhibition of basal and reflex-mediated sympathetic activity in the RVLM by nitric oxide. *Am J Physiol* **268:**R958–R962.

Address correspondence to: Dr. Julie Y. H. Chan, Department of Medical Education and Research, Kaohsiung Veterans General Hospital, Kaohsiung 813, Taiwan, Republic of China. E-mail: yhwa@isca.vghks.gov.tw